

Ultrafast Time-Resolved Laser Spectroscopic Studies of *trans*-Bis(ferrocene-carboxylato)(tetraphenyl-porphyrinato)tin(IV): Intramolecular Electron-Transfer Dynamics[†]

Joon Hee Jang, Hee Jung Kim,[‡] Hee-Joon Kim,[‡] Chul Hoon Kim,[§] Taiha Joo,[§] Dae Won Cho,[#] and Minjoong Yoon^{*}

Department of Chemistry, Chungnam National University, Daejeon 305-764, Korea. *E-mail: mjyoon@cnu.ac.kr

[‡]Department of Applied Chemistry, Kumoh National Institute of Technology, Gumi 730-701, Korea

[§]Department of Chemistry, Pohang University of Science and Technology, Pohang 790-784, Korea

[#]Department of Chemistry, Chosun University, Gwangju 501-759, Korea

Received June 25, 2007

Photophysical properties of a newly-synthesized porphyrin derivative, *trans*-bis(ferrocene carboxylato)-(5,10,15,20-tetraphenylporphyrinato)tin(IV) [Sn(TPP)(FcCOO)₂] were investigated by means of steady-state and fs-time resolved laser spectroscopic techniques, and compared with those of a standard molecule, *trans*-dichloro(5,10,15,20-tetraphenyl-porphyrinato)tin(IV) [Sn(TPP)Cl₂]. The fluorescence spectrum of Sn(TPP)(FcCOO)₂ was observed to exhibit dual emission bands originating from the S₂-state and the S₁-state, which was greatly quenched as compared to those of Sn(TPP)Cl₂. The fs-time resolved fluorescence and transient absorption spectroscopic measurements revealed that the fluorescence quenching is due to formation of the long-lived charge transfer state by intramolecular electron transfer from ferrocene to the S₂-excited SnTPP in addition to the enhanced non-radiative deactivation processes.

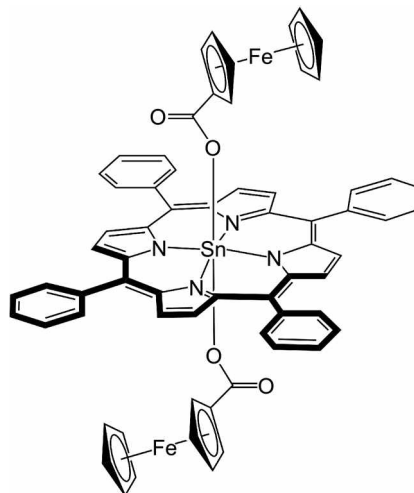
Key Words : Ferrocene-Sn-porphyrin, Photoinduced electron transfer, Ultrafast laser spectroscopy

Introduction

Tin(IV) porphyrins have been attracting much attention because of many advantages in various applications of the particular properties conferred by the highly charged main group metal center.¹ The large Sn(IV) ion can be accommodated in the porphyrin core without distorting the planarity of the macrocyclic ligand. tin(IV) porphyrins are diamagnetic and readily form stable six-coordinate complexes with the *trans*-dialkyl anionic ligands.^{1,2} The preferential coordination of the Tin(IV) porphyrins to oxyanionic ligands has been used to develop the elaborate multiporphyrin arrays³⁻⁷ and porous structures with uniform channels.^{8,9} It has been also applied to develop nano materials¹⁰⁻¹⁴ as the promising photoelectronic materials including photocatalysts¹²⁻¹⁴ and phototherapeutic agents.^{15,16} These applications are based on the excited-state electron transfer between centered metal ion and ligands coordinated to the metal. Actually the photophysical studies of some metal-centered porphyrins have revealed that the higher excited singlet states of porphyrins are important intermediates in the electron transfer. For example, the Zinc porphyrin is well known to exhibit electron donating character in the S₂ state,^{17,18} whereas in case of Sb-porphyrin, S₂-excited state acts as an electron acceptor.¹⁹

However, the photophysical properties of the tin(IV) porphyrins have not been systematically investigated with regard to the excited-state electron transfer as compared to those of other metal-centered porphyrins even though the electrochemical properties have been reported frequently.^{20,21}

In the course of the systematic photophysical studies of tin(IV) porphyrins, we have synthesized a new tin(IV) porphyrin complex, *trans*-bis(ferrocenecarboxylato)(5,10,15,20-tetraphenylporphyrinato)tin(IV) [Sn(TPP)(FcCOO)₂],²² and characterized its molecular structure by X-ray crystallography as shown in Scheme 1. The cyclic voltammetry for Sn(TPP)(FcCOO)₂ exhibits three distinctive redox couples consisting of one oxidative wave and two reductive waves due to the ferrocenecarboxylato ligands and the porphyrin ring, respectively, implying electron transfer between ferrocene and porphyrin. Thus, it is expected that Sn(TPP)(FcCOO)₂ should exhibit the photoelectronic properties, and in this work we examined photophysical properties of the newly synthesized [Sn(TPP)(FcCOO)₂] in conjunction with the electron transfer dynamics by using fs-time resolved



Scheme 1. Molecular structure of Sn(TPP)(FcCOO)₂.

[†]This paper is dedicated to Professor Sang Chul Shim on the occasion of his honorable retirement.

laser spectroscopic techniques as well as steady-state spectral measurements.

Experimental Section

Materials. *Trans*-bis(ferrocenecarboxylato)(meso-tetraphenylporphyrinato)tin(IV)[Sn(TPP)(FcCOO)₂] was synthesized and characterized according to the previously reported procedures.²² *trans*-Dihydroxo(meso-tetraphenylporphyrinato)tin(IV) (100 mg, 0.13 mmol) prepared by the reported procedures²³ and ferrocenecarboxylic acid (59 mg, 0.26 mmol) (Aldrich) were dissolved in anhydrous CH₂Cl₂ (20 mL). The reaction mixture was stirred at room temperature. After 24 h, the solution was filtered through a Celite pad. The solvent of the filtrate was evaporated under reduced pressure to give a crude product. It was then recrystallized from CH₂Cl₂/CH₃CN solution to afford crystalline solids of *trans*-bis(ferrocenecarboxylato)(meso-tetraphenylporphyrinato)tin(IV) (TPP)Sn(FcCOO)₂. The synthesized crystalline solids have been recognized to be (TPP)Sn(FcCOO)₂ by means of IR, UV-visible absorption, ¹H, ¹³C NMR spectroscopy and MALDI-TOF mass spectroscopy as previously reported.²² Yield: 100 mg (66%). ¹H NMR (500 MHz, CDCl₃): δ 9.25 (s, 8H, β-pyrrolic H, ⁴J(SnH) = 14.3 Hz), 8.36 (d, *J* = 6.76 Hz, 8H, *o*-Ph), 7.81 (m, 12H, *m*-Ph), 3.19 (s, 4H, Fc), 2.57 (s, 10H, Fc), 2.13 (s, 4H, Fc). ¹³C NMR (CDCl₃): δ 166.5, 147.3, 141.3, 135.2, 133.0, 128.6, 127.2, 121.8, 74.4, 68.7, 68.5, 68.4. UV-vis (CH₂Cl₂, nm): λ_{max} (log ε) 404 (4.00), 424 (5.16), 521 (2.95), 560 (3.68), 600 (3.41). IR (KBr, cm⁻¹): ν_{CO} 1644. MS (MALDI-TOF): *m/z* 961.08 [(M-O₂CFc)⁺ requires 961.13]. Anal. Calcd. for C₆₆H₄₆N₄O₄Fe₂Sn: C, 66.64; H, 3.90; N, 4.71. Found: C, 66.82; H, 3.48; N, 4.91.

The standard compound, *trans*-dichloro (5,10,15,20-tetraphenylporphyrinato)tin(IV) [Sn(TPP)Cl₂] was also synthesized by the reported procedures.²⁴

Spectroscopic measurements. The UV-visible absorption spectra was recorded on Cary 3E UV-Visible spectrophotometer for toluene solution of (TPP)Sn(FcCOO)₂. The steady-state fluorescence spectra were measured on a scanning SLM-AMINCO 4800 spectrofluorometer.

The ps- or fs-time-resolved fluorescence spectroscopy was performed by using time-correlated single photon counting (TCSPC)^{25, 26} and up-conversion techniques,²⁷ respectively. The excitation source for TCSPC is a self mode-locked Ti:Sapphire laser (Coherent Model MiraTM 900) pumped by Nd:YVO₄ laser (Coherent VerdiTM diode-pumped laser). The laser output has ~200 fs pulse width with a repetition rate, 76 MHz, and it can span the excitation wavelength in the range of 235-300 and 350-490 nm by second- and third-harmonic generations by means of LBO and BBO crystals, respectively. The laser pulse power was minimized to be 1.2 μW/ pulse by passing through pulse picker. The beam area on the sample was about 1.5 mm². All the standard electronics for the TCSPC system were from the Edinburgh Instruments. The instrument function was measured by detecting the scattered laser pulse of ~200 fs with quartz

crystal. The up-conversion set-up is described in detail in the previous report.²⁷ Light source employed for the up-conversion was the output of a home-made cavity-dumped Kerr lens mode-locked Ti:sapphire laser at 820 nm. The repetition rate and pulse energy were adjusted to 500 kHz and 40 nJ. A pump pulse of 410 nm was generated in 200 mm thick LBO crystal. The residual 820 nm output was used as gate pulse. Group velocity dispersion of the gate and the pump pulses were compensated by negative chirped mirrors and fused silica prism pairs. Width (FWHM) of the instrumental response was about 100 fs from the cross correlation measurement with a 500 mm thick BBO crystal. Magic angle detection was used to avoid the effect of polarization.

The transient absorption spectra were measured by using a fs-transient absorption spectroscopic system which have been reported elsewhere.^{28,29} A light source consists of a cw self-mode-locked Ti:sapphire laser (Mira 900 Basic, Coherent) pumped by an Ar⁺ laser (Innova 310, Coherent) and a Ti:sapphire regenerative amplifier system (TR 70, Continuum) with a Q-switched Nd:YAG laser (Surelight I Continuum). The fundamental output from the regenerative amplifier (780 nm, 3-4 mJ/pulse, 170 fs fwhm, 10 Hz) was frequency doubled (390 nm) and used as an excitation light pulse. The energy of the excitation pulse measured with a Joule meter (P25, Scientech) was 33 × 10⁻³ mJ/pulse and its spot diameter on the sample was nearly 1 mm. The shot-to-shot fluctuation of the energy was less than 10%. The residual of the fundamental output was focused into a quartz cell (1 cm path length) containing H₂O to generate a white-light continuum as a probe pulse. Transient absorption intensity was displayed as percentage absorption,²⁹ % A = 100 × (1 - R/R₀), where R and R₀ represent intensity of the light of the probe pulse with and without excitation, respectively. The time resolution of system is less than 1 ps for the sample with a large absorption coefficient at the excitation wavelength.

Results and Discussion

The bis(ferrocenecarboxylato)tin(IV) porphyrin complex Sn(TPP)(FcCOO)₂ was synthesized by the reaction of *trans*-dihydroxo(meso-tetraphenylporphyrinato)tin(IV) complex Sn(TPP)(OH)₂ with two equivalents of ferrocenecarboxylic acid, FcCOOH. The complex Sn(TPP)(FcCOO)₂ was fully characterized by various spectroscopic methods and elemental analysis, and identified to be the same as that reported previously.¹⁹

Figure 1 shows the absorption spectrum of Sn(TPP)(FcCOO)₂ in toluene, which exhibits Soret band around 420 nm and Q-bands at 560 nm and 595 nm. The intensities of these bands are highly hyperchromic (molar absorptivity: ε = 4.0 × 10⁵ M⁻¹·cm⁻¹) with a slight blue shift as compared to those of Sn(TPP)Cl₂ (ε = 1.4 × 10⁵ M⁻¹·cm⁻¹), indicating that FcCOO causes some electronic perturbation of the porphyrinato ligand more effectively than Cl, probably by stronger charge-transfer interaction.³⁰ Upon excitation of the Q-band

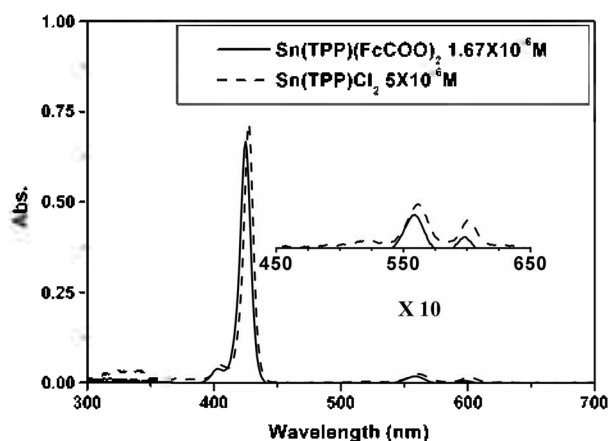


Figure 1. UV-Visible spectra of (TPP)Sn(FcCOO)₂ (solid line) and (TPP)SnCl₂ (dash line) in toluene.

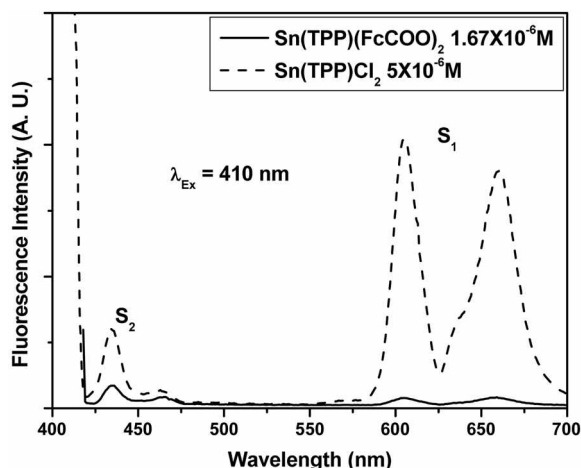


Figure 2. Fluorescence emission spectra of (TPP)Sn(FcCOO)₂ (solid line) and (TPP)SnCl₂ (dash line) in toluene.

of Sn(TPP)(FcCOO)₂ and Sn(TPP)Cl₂, fluorescence due to the S₁ → S₀ transition appeared at 605 and 660 nm. On the other hand, upon excitation of the Soret band at 410 nm, another emission band at 435 nm with a shoulder at 465 nm additionally, which is attributed to the S₂ → S₀ transition. Figure 2 shows the fluorescence spectra measured by adjusting the optical densities of both molecules to be the same at the excitation wavelength, 410 nm in order to estimate the relative fluorescence quantum yield. It is evident from this measurement that both S₁- and S₂-fluorescence intensities of Sn(TPP)(FcCOO)₂ are extraordinarily quenched from those of Sn(TPP)Cl₂. Interestingly, the relative quenching ratio of S₁ fluorescence is much larger (~30 times) than that of S₂ fluorescence (~4 times), implying that deactivation process of S₁ state is more efficient than

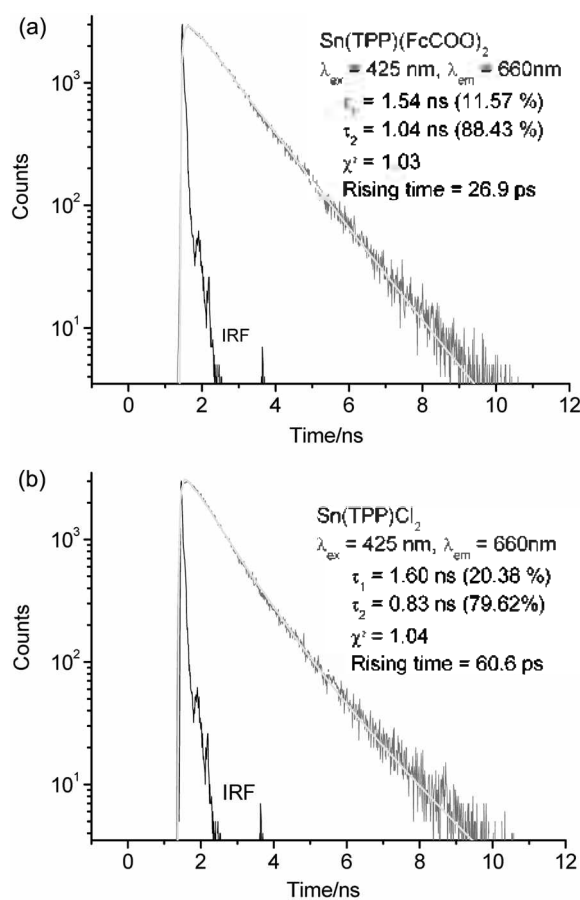


Figure 3. S₁-fluorescence decay profiles of Sn(TPP)(FcCOO)₂ (a) and Sn(TPP)Cl₂ (b) detected at 660 nm.

that of S₂ state. In order to explore the deactivation processes in detail, the S₁- and S₂- fluorescence lifetimes of both porphyrins are measured by TCSPC and up-conversion techniques, respectively. Figure 3 shows the typical S₁-fluorescence decay profiles of Sn(TPP)(FcCOO)₂ and Sn(TPP)Cl₂ detected at 660 nm with excitation at 425 nm, fitting to biexponential function, from which two decay times (0.8–1.6 ns) originating from two vibronic states. The decay times were summarized in Table 1. The S₂-fluorescence decay profiles of Sn(TPP)(FcCOO)₂ and Sn(TPP)Cl₂ were also measured by means of up-conversion method and illustrated in Figure 4, from which S₂-state lifetimes of Sn(TPP)(FcCOO)₂ and Sn(TPP)Cl₂ were determined to be 240 fs and 384 fs, respectively. Although S₂ emission life time of Zn-, Cd-, Al- and Sb-centered TPP have been reported,^{19,31} This is the first observation of S₂ emission for Sn centered porphyrin. As seen in Table 1, the fluorescence decay times of Sn(TPP)(FcCOO)₂ are slightly different from

Table 1. S₁- and S₂-state properties (λ_{S1}, λ_{S2}, τ_{S1}, τ_{S2}), oxidation and reduction potentials of Sn(TPP)(FcCOO)₂ and Sn(TPP)Cl₂

	λ _{S1}	λ _{S2}	τ _{S1}	τ _{S2}	E _{OX} ^o	E _{Red} ^o	
Sn(TPP)(FcCOO) ₂	605 nm	434 nm	1.04 ns (88.4%)	1.54 ns (11.6%)	240 fs	0.11 V	-1.47 V
Sn(TPP)Cl ₂	606 nm	434 nm	0.83 ns (79.6%)	1.60 ns (20.4%)	384 fs	–	–

^ovs. SCE; Ref. 22.

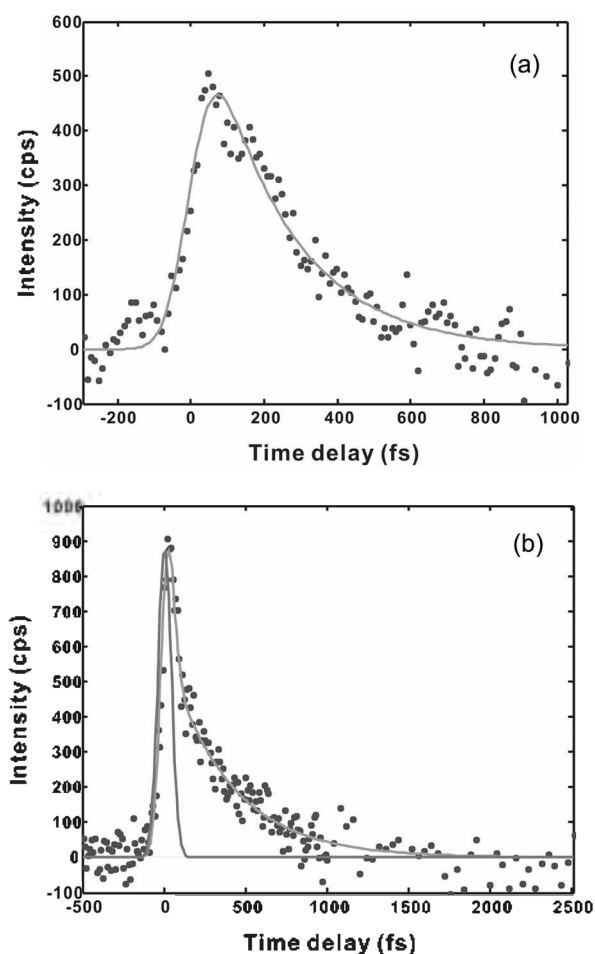


Figure 4. S_2 -fluorescence decay profiles of $\text{Sn}(\text{TPP})(\text{FcCOO})_2$ (a) and $\text{Sn}(\text{TPP})\text{Cl}_2$ (b) measured by up-conversion technique. $\lambda_{\text{ex}} = 410$ nm.

those of $\text{Sn}(\text{TPP})\text{Cl}_2$ in spite of the extraordinarily lower fluorescence quantum yield of $\text{Sn}(\text{TPP})(\text{FcCOO})_2$ as compared with that of $\text{Sn}(\text{TPP})\text{Cl}_2$. This indicates that there is an additional deactivation process of the S_1 - and S_2 -states of $\text{Sn}(\text{TPP})(\text{FcCOO})_2$ to the radiative and nonradiative processes such as internal conversion and intersystem crossing. It is known that the excited SnTPP works as an electron acceptor^{14, 32} as in the case of SbTPP , and the additional deactivation process in the excited states of $\text{Sn}(\text{TPP})(\text{FcCOO})_2$ should be an intramolecular electron transfer from FcCOO to the excited SnTPP , forming an excited charge transfer state (CS). Supporting this speculation, the free energy changes for the intramolecular electron transfer (ΔG_{ET}) via the S_1 or S_2 states can be estimated to be -0.30 and -1.34 eV, respectively, according to the following Rehm-Weller equation 1,

$$(\Delta G_{\text{ET}}) = E_{\text{ox}} - E_{\text{red}} - E_{S_1 \text{ or } S_2} \quad (1)$$

where $E_{S_1 \text{ or } S_2}$ is the S_1 - or S_2 -state energy of $\text{Sn}(\text{TPP})(\text{FcCOO})_2$ estimated from the peak position of the S_1 or S_2 fluorescence, and E_{ox} and E_{red} are the oxidation and reduction potentials of $\text{Sn}(\text{TPP})(\text{FcCOO})_2$ listed in Table 1. The $-\Delta G_{\text{CS}}$'s are in good correlation with measured lifetimes

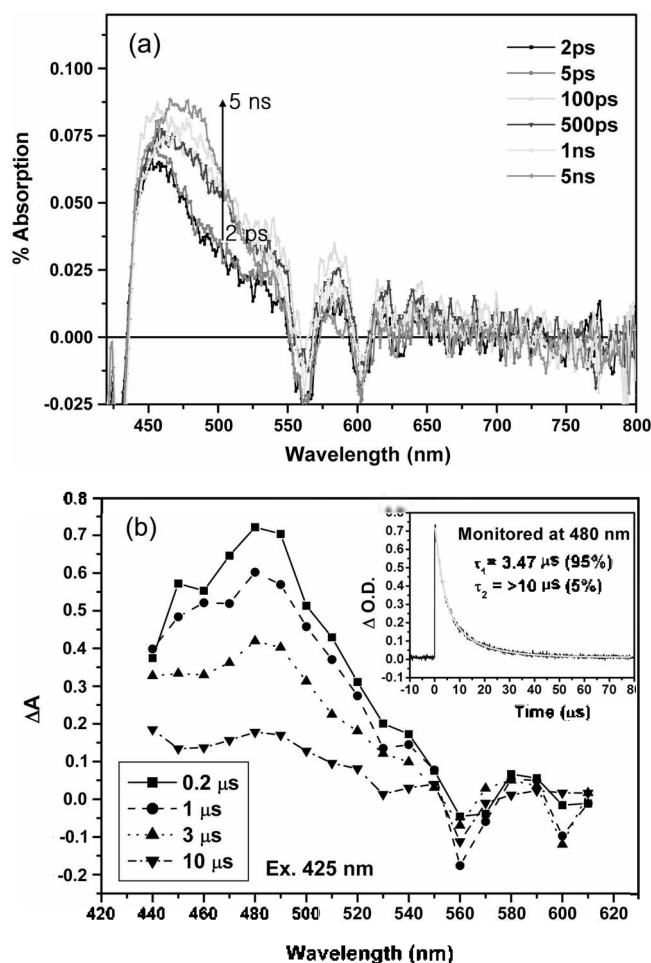


Figure 5. fs-Transient absorption spectra ($\lambda_{\text{ex}} = 390$ nm) (a) and ns-transient absorption spectra with decay profile of 480 nm transient band (inset) (b) of $(\text{TPP})\text{SnCl}_2$.

of the excited states; the shorter the lifetimes, the larger the $-\Delta G_{\text{CS}}$ values, indicating that the intramolecular electron transfer is more favorable via the S_2 state than via the S_1 state.

In order to examine formation of the CS, fs-transient absorption spectra of $\text{Sn}(\text{TPP})\text{Cl}_2$ and $\text{Sn}(\text{TPP})(\text{FcCOO})_2$ in toluene were measured. Figure 5(a) shows development and decay of the transient absorption spectra of $\text{Sn}(\text{TPP})\text{Cl}_2$ as a function of decay time upon excitation at 390 nm. Immediately after excitation, the transient absorption band at 450 nm appeared with a shoulder around 520 nm as well as the negative absorption bands at 560 and 595 nm due to bleaching of the Q-bands. The 450 nm band disappears after 5 ps, followed by enhancement of the 520 nm shoulder which remains for ~ 1 ns, indicating that the 450 nm and 520 nm band are attributed to the S_2 and S_1 states, respectively. Also another band appears at 480 nm from 500 ps which remains over 5 ns, and it can be attributed to triplet state formed by intersystem crossing from the S_1 state as confirmed by the nano-second transient absorption spectrum as shown in Figure 5(b) exhibiting its decay time of $3.47 \mu\text{s}$. These observations indicate that the intersystem crossing is the main deactivation process of the excited singlet states of

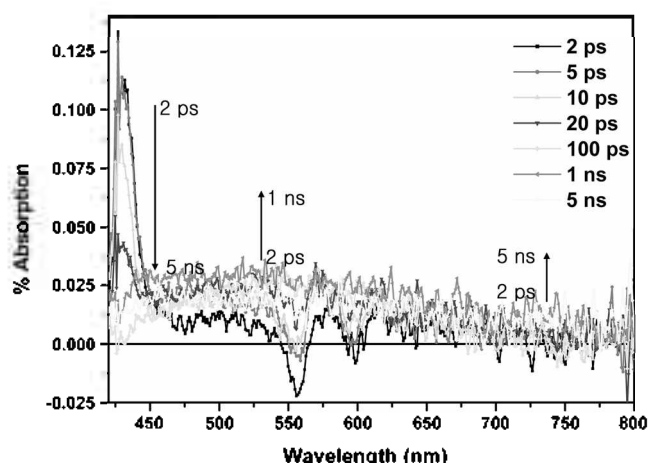


Figure 6. fs-Transient absorption spectra of $\text{Sn}(\text{TPP})(\text{FcCOO})_2$ upon excitation at 390 nm.

SnTPPCl_2 . The fs-transient absorption spectral features of $\text{Sn}(\text{TPP})(\text{FcCOO})_2$ also exhibits the S_2 -absorption band at 435 nm with the S_1 -absorption band at 520 nm (Figure 6) as in the case of SnTPPCl_2 . However, it is noteworthy that the decay of the S_2 state is observed to be accompanied with enhancement of the broad transient band around 680 nm, which is not observed from the transient absorption spectra of $\text{Sn}(\text{TPP})\text{Cl}_2$. The transient bands around 680 nm can be attributed to the reduced SnTPP , i.e. SnTPP^* as usually observed from many other porphyrin radicals,^{12,14,19} indicating formation of the intramolecular CS, $[\text{Sn}(\text{TPP})^-(\text{FcCOO})_2^{+}]$ formed by the intramolecular electron transfer from FcCOO to the S_2 state of SnTPP as in the case of $\text{Sb}(\text{TPP})$ derivatives.¹⁹ Based on assumption that radiative and nonradiative rate constants of $\text{Sn}(\text{TPP})(\text{FcCOO})_2$ are the same as those of $\text{Sn}(\text{TPP})\text{Cl}_2$, the rate constant of the CS formation (k_{CS}) via S_2 state can be related to the S_2 fluorescence lifetimes according to eq. 2,

$$k_{\text{CS}} = 1/\tau_{S_2, \text{Sn}(\text{TPP})(\text{FcCOO})_2} - 1/\tau_{S_2, \text{Sn}(\text{TPP})\text{Cl}_2} \quad (2)$$

where $\tau_{S_2, \text{Sn}(\text{TPP})(\text{FcCOO})_2}$ and $\tau_{S_2, \text{Sn}(\text{TPP})\text{Cl}_2}$ are the S_2 fluorescence lifetimes of $\text{Sn}(\text{TPP})(\text{FcCOO})_2$ and $\text{Sn}(\text{TPP})\text{Cl}_2$, respectively, and it was estimated to be $1.57 \times 10^{12} \text{ s}^{-1}$. The quantum efficiency of CS formation was also estimated to be 0.40 according to the following eq. 3.

$$\Phi_{\text{CS}} = (1/\tau_{S_2, \text{Sn}(\text{TPP})(\text{FcCOO})_2} - 1/\tau_{S_2, \text{Sn}(\text{TPP})\text{Cl}_2}) / (\tau_{S_2, \text{Sn}(\text{TPP})(\text{FcCOO})_2}) \quad (3)$$

The estimated k_{CS} and Φ_{CS} confirm the efficient CS formation of $\text{Sn}(\text{TPP})(\text{FcCOO})_2$ via the S_2 state even in nonpolar solvent, despite the short lifetime of the S_2 state. Furthermore, the 680 bands remains up to 1 ns (Figure 6) which is much longer than the disappearance time of CS of $\text{Sb}(\text{TPP})$ derivatives,¹⁹ indicating that the charge recombination of the CS of $\text{Sn}(\text{TPP})(\text{FcCOO})_2$ is relatively slow. Consequently, it is evident that the fluorescence quenching of $\text{Sn}(\text{TPP})(\text{FcCOO})_2$ is resulted from CS formation by the intramolecular electron transfer from FcCOO to the S_2 -excited $\text{Sn}(\text{TPP})$ in addition to the nonradiative processes

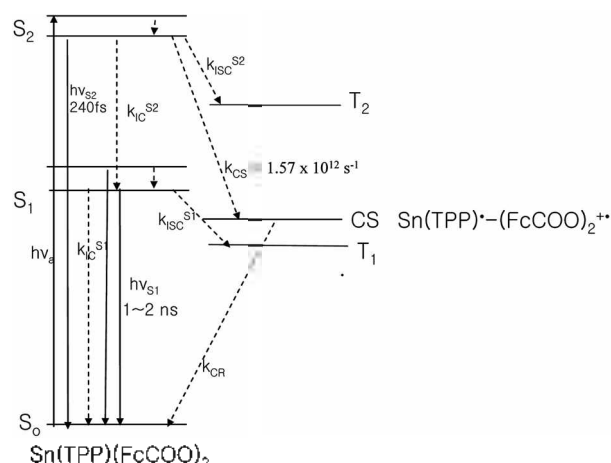


Figure 7. Schematic energy diagram for the deactivation processes in competition with the S_1 - and S_2 -fluorescence ($h\nu_{S_1}$, $h\nu_{S_2}$) of $\text{Sn}(\text{TPP})(\text{FcCOO})_2$ including CS formation and charge recombination (CR) with internal conversion (IC) and intersystem crossing (ISC).

such as internal conversion (IC) and intersystem crossing (ISC). Similarly, the k_{CS} and Φ_{CS} via the S_1 state were estimated to $2.4 \times 10^6 \text{ s}^{-1}$ and $\sim 10^{-4}$, respectively, which are too small to be competitive with the radiative transition from the S_1 -state, indicating that the CS via the S_2 -state is negligible. Furthermore, the decay times of the S_1 -state of $\text{Sn}(\text{TPP})(\text{FcCOO})_2$ are almost the same as those of $\text{Sn}(\text{TPP})\text{Cl}_2$ in spite of the large fluorescence quenching, indicating that quenching of the S_1 -fluorescence may be caused by increase of the ISC or IC rate due to enhanced vibration of the porphyrin ring ligated with the larger ligand.

From these results, the photophysical behavior of $\text{Sn}(\text{TPP})(\text{FcCOO})_2$ may be summarized by the schematic energy diagram. (Figure 7). Upon excitation to the S_2 state, both S_1 and S_2 fluorescence emissions ($h\nu_{S_1}$ and $h\nu_{S_2}$) are generated in competition with formation of CS in addition to the fundamental nonradiative processes. Particularly the radiative decay time of S_2 state was estimated to be 240 fs which was shorter than that of $\text{Sn}(\text{TPP})\text{Cl}_2$ (384 fs) because of the additional rapid CS process by the intramolecular electron transfer from FcCOO to the S_2 state of SnTPP . On the other hand, the radiative decay times of the S_1 state was not much changed, and the additional CS formation via the S_1 state is negligible but the nonradiative rate constants would be increased by the axial ligation with FcCOO so that the S_1 fluorescence is quenched.

Conclusion

In this work, the S_1 - and S_2 -fluorescences of $\text{Sn}(\text{TPP})\text{Cl}_2$ were observed to be greatly quenched by substituting Cl with FcCOO . The fluorescence quenching was found to be due to additional deactivation process to the fundamental non-irradiative relaxation such as internal conversion and intersystem crossing. The additional deactivation process is to form the charge transfer state (CS) very efficiently via

intramolecular electron transfer from FcCOO to the S₂ state of Sn(TPP) as well as the S₁ state as confirmed by the fs-transient absorption spectroscopy as well as the fs-fluorescence spectroscopy. The rapidly formed CS is also found to be unusually stable for 1 ns, indicating that Sn(TPP)-(FcCOO)₂ is probably useful for the molecular photoelectronic devices.

Acknowledgement. This work has been partly supported by the Korea Science and Engineering Foundation (R01-2004-000-10446-0). H-JK and HJK acknowledge Kumoh National Institute of Technology and the Program for the Training of Graduate Students in Regional Innovation conducted by the Korean Ministry of Commerce Industry and Energy, respectively.

References

1. Arnold, D. P.; Block, J. *Coord. Chem. Rev.* **2004**, *248*, 299.
2. Sanders, J. K. M.; Bampos, N.; Clyde-Watson, Z.; Darling, S. L.; Hawley, J. C.; Kim, H.-J.; Mak, C. C.; Webb, S. J. In *The Porphyrin Handbook*, Vol. 3; Kadish, K. M.; Smith, K. M.; Guillard, R., Eds.; Academic Press: San Diego, **2000**; p 1.
3. Kim, H.-J.; Bampos, N.; Sanders, J. K. M. *J. Am. Chem. Soc.* **1999**, *121*, 8120.
4. Redman, J. E.; Feeder, N.; Teat, S. J.; Sanders, J. K. M. *Inorg. Chem.* **2001**, *40*, 2486.
5. Kumar, A. A.; Giribabu, L.; Reddy, D. R.; Maiya, B. G. *Inorg. Chem.* **2001**, *40*, 6757.
6. Langford, S. J.; Woodward, C. P. *Collect. Czech. Chem. Commun.* **2004**, *69*, 996.
7. Hunter, C. A.; Tomas, S. *J. Am. Chem. Soc.* **2006**, *128*, 8975.
8. Fallon, G. D.; Lee, M. A.-P.; Langford, S. J.; Nichols, P. J. *Org. Lett.* **2002**, *4*, 1895.
9. Kim, H.-J.; Jo, H. J.; Kim, J.; Kim, S.-Y.; Kim, D.; Kim, K. *Cryst. Eng. Comm.* **2005**, *7*, 417.
10. Song, Y.; Yang, Y.; Medforth, C. J.; Pereira, E.; Singh, A. K.; Xu, H.; Jiang, Y.; Brinker, C. J.; Van Swol, F.; Shelnut, J. A. *J. Am. Chem. Soc.* **2004**, *126*, 635.
11. Wang, H.; Song, Y.; Medforth, C. J.; Shelnut, J. A. *J. Am. Chem. Soc.* **2006**, *128*, 9284.
12. Moghadam, M.; Tangestaninejad, S.; Mirkhani, V.; Shaibani, R. *Tetrahedron* **2004**, *60*, 6105.
13. Handman, J.; Harriman, A.; Porter, G. *Nature* **1984**, *307*, 534.
14. Jang, J. H.; Jeon, K.-S.; Oh, S.; Kim, H.-J.; Asahi, T.; Masuhara, H.; Yoon, M. *Chem. Mater.* **2007**, *19*, 1984.
15. Philippova, T. O.; Galkin, B. N.; Golovenko, N. Y.; Zhilina, Z. I.; Vodzinskii, S. V. *J. Porph. Phthal.* **2000**, *4*, 243.
16. Embleton, M. L.; Nair, S. P.; Cookson, B. D.; Wilson, M. *J. Antimicrob. Chemother.* **2002**, *50*, 857.
17. Chosrowjan, H.; Taniguchi, S.; Okada, T.; Takagi, S.; Arai, T.; Tokumaru, K. *Chem. Phys. Lett.* **1995**, *242*, 644.
18. Mataga, N.; Shibata, Y.; Chosrowjan, H.; Yoshida, N.; Osuka, A. *J. Phys. Chem. B* **2000**, *104*, 4001.
19. Fujitsuka, M.; Cho, D. W.; Shiragami, T.; Yasuda, M.; Majima, T. *J. Phys. Chem. B* **2006**, *110*, 9368.
20. Chaniotakis, N. A.; Park, S. B.; Meyerhoff, M. E. *Analytical Chemistry* **1989**, *61*, 566.
21. Santos, E. M. G.; Araujo, A. N.; Couto, C. M. C. M.; Montenegro, M. C. B. S. M. *Electroanalysis* **2005**, *17*, 1945.
22. Kim, H. J.; Jeon, W. S.; Lim, J. H.; Hong, C. S.; Kim, H.-J. *Polyhedron* **2007**, *26*, 2517.
23. Crossley, M. P.; Thordarson, P.; Wu, R. A. S. *J. Chem. Soc., Perkin Trans. I* **2001**, 2294.
24. Jiang, J.; Jin, X.; Li, C.; Gu, Z. *J. Coord. Chem.* **1995**, *35*, 313.
25. Kim, Y.; Yoon, M.; Kim, D. *J. Photochem. Photobiol. A : Chem.* **2001**, *138*, 167.
26. Choi, C.-S.; Jeon, K.-S.; Lee, K.-H.; Yoon, M.; Kwak, M.; Lee, S. W.; Kim, I. T. *Bull. Korean Chem. Soc.* **2006**, *27*, 1601.
27. Yoon, M.-C.; Jeong, D. H.; Cho, S.; Kim, D.; Rhee, H.; Joo, T. *J. Chem. Phys.* **2003**, *118*, 164.
28. Furube, A.; Asahi, T.; Masuhara, H.; Yamashita, H.; Anpo, M. *J. Phys. Chem. B* **1999**, *103*, 3120.
29. Asahi, T.; Furube, A.; Fukimura, H.; Ichikawa, M.; Masuhara, H. *Rev. Sci. Instrum.* **1998**, *69*, 361.
30. Buchler, J. W. In *The Porphyrins*; Dolphin, D., Ed.; Academic Press: New York, **1978**; Volume I, Chapter 10.
31. Ohkubo, K.; Santic, P. J.; Tkachenko, N. V.; Lemmetyinen, H.; Wenbo, E.; Ou, Z.; Shao, J.; Kadish, K. M.; Crossley, M. J.; Fukuzumi, S. *Chem. Phys.* **2006**, *326*, 3.
32. Kadish, K. M.; Xu, Q. Y.; Maiya, G. B.; Barbe, J.-M.; Guillard, R. *J. Chem. Soc., Dalton Trans.* **1989**, 1531.
33. Tokumaru, K. *J. Porph. Phthal.* **2001**, *5*, 77.